

Article

Effect of Internal Moisture and Outer Relative Humidity on Concrete Carbonation

Charlotte Thiel ^{1,*}, Johanna Kratzer ², Benedikt Grimm ³, Thomas Kränkel ³ and Christoph Gehlen ³¹ OTH Regensburg, 93053 Regensburg, Germany² Ingenieurbüro Grassl GmbH, 20537 Hamburg, Germany³ Centre for Building Materials, Technical University of Munich, 81245 Munich, Germany

* Correspondence: charlotte.thiel@oth-regensburg.de; Tel.: +49-941-943-1349

Abstract: With steadily rising CO₂ concentrations in the ambient air and fast-changing concrete compositions with reduced clinker contents, the availability of reliable and accelerated concrete carbonation tests is of crucial importance to design durable structures. This paper focuses on the effects of moisture under accelerated conditions and the effects of different CO₂ exposure conditions. Mortar prisms incorporating three different cement types were cured and stored at either 50% or 65% relative humidity (RH). Afterwards, the prisms were carbonated at different ambient humidities (50, 57 and 65%), different CO₂ concentrations (0.04, 1 and 3 vol.%) and complemented by a series of tests at increased gas pressure (2 barg). High-resolution test methods were used to explain the underlying carbonation mechanisms. The results show that pre-conditioning for two weeks—as currently suggested by the European Standard—seems to be too short because the initial inner moisture content severely affects the carbonation rate. Relative humidity during carbonation of 57% led to higher carbonation rates compared to 50% and 65%. In addition, climate data needs to be periodically (preferably permanently) recorded in research experiments and in laboratory testing to ensure fair interpretation of experimental results.

Keywords: accelerated carbonation; concrete; moisture; durability; relative humidity

Citation: Thiel, C.; Kratzer, J.; Grimm, B.; Kränkel, T.; Gehlen, C. Effect of Internal Moisture and Outer Relative Humidity on Concrete Carbonation. *CivilEng* **2022**, *3*, 1039–1052. <https://doi.org/10.3390/civileng3040058>

Academic Editor: Akanshu Sharma

Received: 15 September 2022

Accepted: 7 November 2022

Published: 17 November 2022

Publisher's Note: MDPI stays neutral with regard to jurisdictional claims in published maps and institutional affiliations.



Copyright: © 2022 by the authors. Licensee MDPI, Basel, Switzerland. This article is an open access article distributed under the terms and conditions of the Creative Commons Attribution (CC BY) license (<https://creativecommons.org/licenses/by/4.0/>).

1. Introduction

Concrete carbonation is still a crucial field of research. On the one hand, CO₂ is absorbed from the atmosphere, reducing the global warming potential of concrete (see [1]). On the other hand, carbonation might significantly reduce the durability of reinforced concrete structures due to lowering the pH value of the pore solution and thus increasing the risk of reinforcement corrosion. Under natural conditions, carbonation progress is very slow due to the low CO₂ content in the atmosphere. Therefore, testing the carbonation resistance of concrete at an atmospheric concentration of CO₂ takes a significant amount of time. With the introduction of DIN EN 12390-12:2020-04 [2], the accelerated carbonation procedure is regulated by applying an increased CO₂ concentration of 3 ± 0.5% by volume at atmospheric pressure (1.013 mbar at 25 °C) and 20 ± 2 °C at a relative humidity of 57 ± 3%. For the accelerated carbonation test, samples are cured for 28 d at room temperature under water, pre-stored for 14 d under natural carbonation exposure (laboratory air conditions) and then carbonated for up to 70 days under accelerated conditions. The carbonation progress is measured after 7, 28 and 70 days. As this procedure deviates from existing international regulation and standards, the effects of pre-storage and ambient conditions during carbonation is further investigated here.

When CO_{2,g} diffuses inside the air-filled pore structure, carbonic acid is formed with water and a reaction with different phases of the hardened cement paste takes place [3,4].

Different parameters affect carbonation (Figure 1). Note that the concrete quality changes with time. As the binder type, CO₂ concentration, pressure and relative humidity are further investigated, they are discussed shortly, in the following.

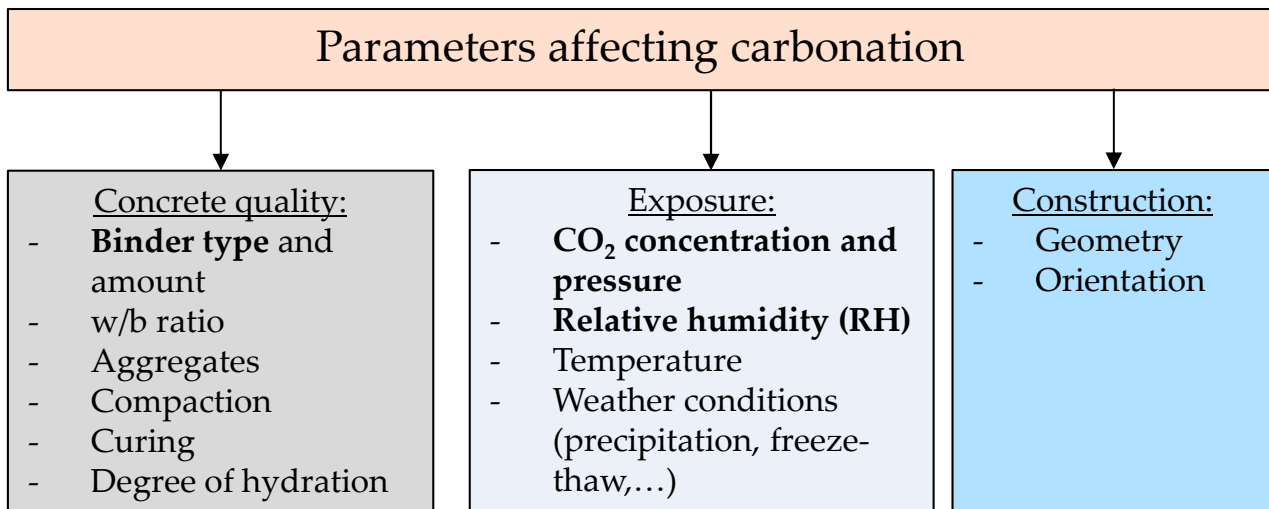


Figure 1. Parameters affecting the carbonation propagation of cementitious materials. Here, only the bold parameters marked in grey are investigated and therefore explained in more detail.

Concerning the type of binder, the main parameters affecting carbonation are the binder-specific alteration of the pore structure, the exact chemistry of the phase composition, the degree of hydration, and the water retention. Consequently, indirect test methods (compressive strength, permeability, etc.) show no or minor correlation to the carbonation resistance [3], which is why direct performance tests are required.

Increasing the CO₂ concentration should theoretically lead to higher carbonation rates only depending on the CO₂-concentrations; Equation (1):

$$B_{K, \text{ theor}} = \frac{d_S}{d_N} = \frac{K_S}{K_N} = \sqrt{\frac{[\text{CO}_2]_S}{[\text{CO}_2]_N}} \quad (1)$$

$B_{K, \text{ theor}}$	Theoretical acceleration factor;
d_N, d_S	Carbonation depth under natural („N”) and accelerated (“S”) conditions;
K_N	Carbonation coefficient under natural conditions [mm/d ^{0.5}]; $K_N = K\sqrt{[\text{CO}_2]_N}$;
K_S	Carbonation coefficient under accelerated conditions [mm/d ^{0.5}]; $K_S = K\sqrt{[\text{CO}_2]_S}$;
$[\text{CO}_2]_N$	Natural CO ₂ -concentration [vol.%];
$[\text{CO}_2]_S$	Accelerated CO ₂ -concentration [vol.%].

However, the experiments show that increasing the CO₂ concentration leads to a higher deviation from the theoretical acceleration. To compensate for that, Gehlen suggests a conversion factor of 1.25 for experiments at 2 vol.% [5]. Furthermore, Hunkeler et al. determined correction factors of 1.17 and 1.36 for 1 and 4%, respectively [6]. Theoretically, the phase formation is independent of the CO₂ concentration. However, the formation of vaterite and aragonite was found to be favored by accelerated carbonation [4]. Furthermore, the carbonation of C-S-H might be favored by accelerated carbonation [7] and increased moisture release might also have a retarding effect on the accelerated carbonation [6]. However, there is a general census that accelerated carbonation is possible and does not change the ranking of different concrete compositions [3,6,8].

The accelerated carbonation is less common due to increased ambient pressure. Under natural conditions, overpressure exists, for example, in civil engineering structures, such as landfills for nuclear waste [9]. According to Zou et al. [10] overpressure can likewise be caused by wind, although an effect can only be observed above an average velocity of 6 m/s and is amplified by fluctuating currents. During overpressure, CO₂ transport occurs by both diffusion and advection.

For concrete carbonation to occur, moisture is needed for CO_2 to form carbonic acid. Steiner et al. studied the carbonation of C-S-H, portlandite and ettringite at 57% and 91% RH [11,12]. C-S-H carbonation is significantly faster at high RH (91% compared to 57%), while portlandite carbonates only partly at 57% RH and the formation of metastable vaterite and aragonite is promoted at RH of 57%, while at 91% calcite was directly produced. On the other hand, the diffusion coefficient D_c of CO_2 is severely reduced with increasing RH. D_c in water is $0.8 \cdot 10^{-12} \text{ m}^2/\text{s}$ to $5 \cdot 10^{-12} \text{ m}^2/\text{s}$, while in air-filled pores D_c is up to $1.5 \cdot 10^{-8} \text{ m}^2/\text{s}$. Consequently, the optimal carbonation speed under natural conditions is between 50 and 70% RH [13].

For accelerated conditions, Papadakis [14], Leemann et al. [15], Russel et al. [16], De Ceukelaire [17] and Elsalamawy et al. [18] carried out experiments at different pre-conditioning and different carbonation conditions. This makes a direct comparison of these studies difficult or even impossible. However, the optimal RH for carbonation seems to be around 50% as 70% already led to reduced carbonation rates. Therefore, the current paper chose RH of 50%, 57% and 65% to identify the optimum carbonation conditions in the range of 50% to 70% RH. Furthermore, current standards suggest CO_2 concentrations between 0.04 (natural) and 50 vol.% (in France) [19] while varying pre-conditioning and RH during carbonation. Soja et al. [20] showed a change in microstructure due to drying at moderate relative humidities without carbonation and highlighted the importance of separating drying effects from carbonation effects on the microstructure. As RH during pre-conditioning might affect the carbonation results and differs in research and standard tests mainly between 50 and 65% RH, this range was chosen for the experiments on pre-conditioning.

2. Materials and Methods

2.1. Materials and Pre-Storage

All experiments were carried out on mortar prisms incorporating three different cement types (see Table 1). As the w/b ratio directly affects the diffusion and thus the carbonation rate, all mixes had an equal w/b ratio. Note that the water/clinker ratio is different in the mixes. With the aim of generating clearly measurable carbonation depths and, at the same time, covering the normative range, the limit value recommended in EN 206:2021-06 [21] for XC3 of w/c = 0.55 was chosen. A fine aggregate (0/2) complemented the mortar mixtures (water/sand ratio = 0.234).

Table 1. Mortar types and properties.

Cement Type	Cement Label	Air Content ¹	Consistency ²	Mortar Density Fresh State/28 d	28 d Compressive/ Tensile Strength	Mixture Label
	[-]	[vol.%]	[mm]	[kg/m ³]	[MPa]	[-]
OPC	CEM I 42.5 N	1.9	192	2200/2210	57.6/7.7	M1
Portland Composite Cement (with limestone filler)	CEM II A-LL 42.4 N	1.5	246	2180/2230	41.7/6.7	M2
Granulated blast furnace slag cement	CEM II/B 42.5 N	1.5	226	2180/2150	51.4/7.2	M3

¹ Determined with an Air Entrainment Pressure Balance Meter according to DIN EN 12350-7:2019-09. ² Determined with the Haegermann equipment according to DIN EN 1015-3, Mai 2007.

From each mortar composition, prisms ($160 \times 40 \times 40 \text{ mm}^3$) were cast (Figure 2a), covered with a moist burlap cloth and demolded after 1 d. From each series, three prisms were cast with a metal tube (diameter of 5 mm) in the middle and at a height of 35 mm to replace the tube later with an RH sensor (Figure 2b).

Prisms from M1, M2 and M3 were used to determine the effect of RH during pre-conditioning and accelerated carbonation (3 vol.% CO_2 concentration). Additional prisms of the M2 mix were used to further investigate the effect of different carbonation impacts (1 vol.% CO_2 concentration and the addition of pressure and natural carbonation up to 84 d).

After demolding, the prisms were cured for another 27 d in a lime-saturated solution at 20 ± 0.5 °C. This long curing period was chosen to study the effect of RH while minimizing the effect of ongoing hydration during the experiments. The prisms were then stored in argon flooded, ventilated chambers at 20 ± 0.5 °C and RH of either 50% or 65%, respectively, for another 12 d. To reach equilibrium conditions over the whole specimen height, the samples were then sealed with cling film and dried for 48 h at 40 °C, unsealed and re-stored at either 50% or 65% RH, respectively, for at least another 21 d (age 42 d). This procedure aimed to moderately dry the core of the specimens. The pre-conditioning was carried out in a CO₂-free atmosphere. In addition to filling the chambers with argon, KOH pellets were placed inside the chambers as CO₂ catchers.

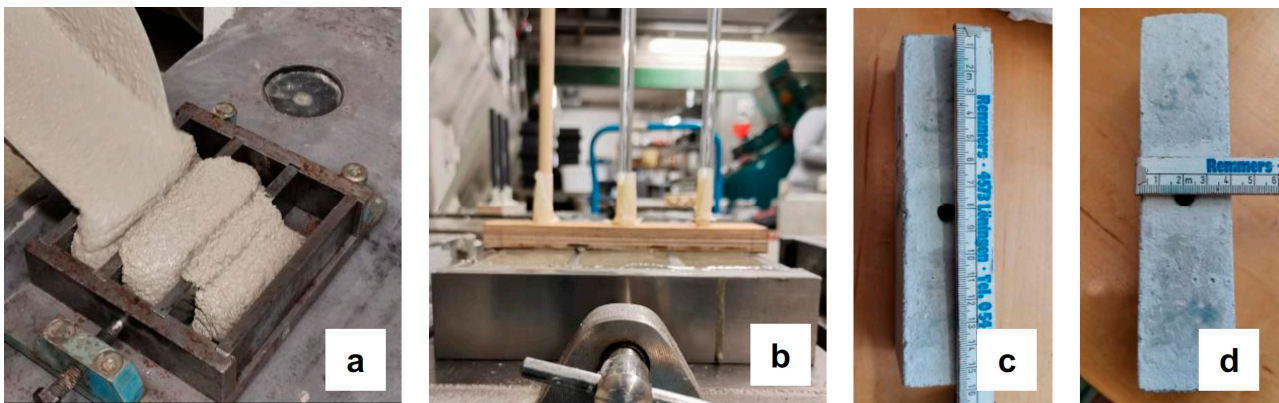


Figure 2. (a): Manufacture of test specimen; (b) tubes as placeholders for humidity sensors; (c,d): mortar prism with recess for humidity sensors.

RH sensors (FHAD 46-C2 from Ahlborn) were placed inside different specimens after curing and data on temperature and RH were logged every 5 min. Figure 3 shows the measurements of RH during pre-storage of 7 w after the samples were intermittent dried at 40 °C at the age of 21 d. The inner RH is not significantly changing. However, instead of 65% outer RH, 61%, 50% and 57% were measured, indicating that there is only minor difference in the RH inside the samples.

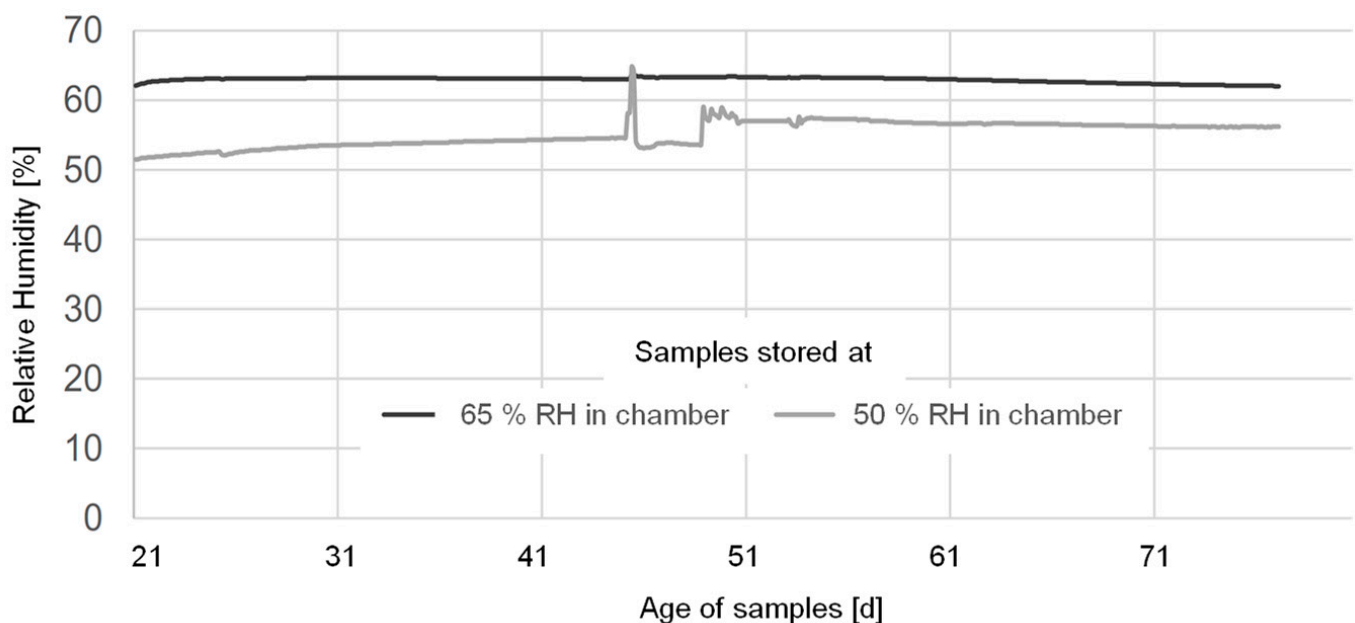


Figure 3. Internal relative humidity during CO₂-free storage at 20 °C and 50% and 65% RH, respectively.

2.2. Carbonation Exposure

Natural carbonation was carried out at $20 \pm 1 \text{ }^\circ\text{C}$ and $65 \pm 2\%$ RH and 0.04% CO_2 . The CO_2 concentration was only selectively measured but showed rather constant values of 0.04% excluding times when the chamber was opened and up to 4 h after placing the first samples where the concentration was lower.

Accelerated carbonation was carried out at $20 \pm 1 \text{ }^\circ\text{C}$, either $50, 57$ or $65 \pm 2\%$ RH and 1 ± 0.05 or $3 \pm 0.05\%$ CO_2 . In addition, one series was carbonated under 2 barg overpressure ($=3 \text{ bar}$) using the autoclave HR-28L of Berghof (Figure 4 left). The autoclave was modified to measure CO_2 concentration, RH and temperature.

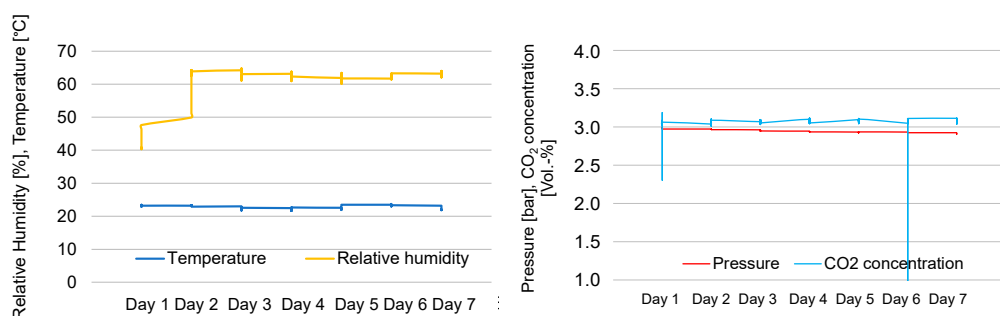


Figure 4. (Left): Autoclave HR-28L of the company Berghof; (Middle): RH, Temperature; (Right): Pressure and CO_2 concentration during accelerated carbonation at planned conditions of 2 barg ($=3 \text{ bar}$), $20 \text{ }^\circ\text{C}$ and $3 \text{ vol.}\% \text{CO}_2$.

The ambient conditions were regularly monitored (Figure 4 middle and right). The temperature was on average $22.6 \text{ }^\circ\text{C}$, total pressure 2.9 bar , CO_2 concentration $3.1 \text{ vol.}\%$ and RH 61.6% .

2.3. Methods

Table 2 shows the measurements that were regularly undertaken.

Table 2. Summary of Methods.

Method	Aim of Method	Preparation	Description	Reference
Color indicator spray test	Determination of carbonation depth	Lateral breaking of prisms, dry cleaning of dust	Spraying color indicator solution on freshly broken surfaces; 5 readings were taken per side	[2,22,23]
Capillary suction	Information on change in capillary porosity on the surface	Drying at $40 \text{ }^\circ\text{C}$ for 7 d Lateral sealing	Specimens are placed on spacers of 5 mm in demineralized water with a height of $7 \pm 1 \text{ mm}$	[24,25]
Mercury intrusion porosimetry (MIP)	Determination of total porosity and pore size distribution (1.7 nm to 0.5 mm)	(Carbonated) edge zone was cut, solvent exchange method was used and samples with visually low amount of aggregates were used	Mercury is injected into the sample under increasing pressure. The total porosity is determined from the total intruded volume. The pore size distribution is determined by the amount of mercury intruded at a given pressure level	[26,27]
Thermo-gravimetric analysis (TGA)	Determination of chemical changes due to carbonation	Same as for MIP, the broken pieces were fine-grinded	Changes of mass are determined as a function of the heating temperature	[7,28,29]

The color spray test is an indirect but very fast and easy method to determine the carbonation depth [22,30]. The carbonation depth was indirectly determined by 0.1 phenolphthalein solution. According to [31], the turnover range for phenolphthalein (solution with a concentration of 1%) from red to colorless is between pH 8.2 and pH 9.8. The readings were taken 60 ± 5 min after spraying on all four sides every 5 mm up to 10 mm to the edge. Consequently, five points were taken per side, resulting in twenty measurements per age and prism.

CO₂ diffuses through the capillary pore system into the samples at the selected relative humidities. The determination of capillary suction is therefore a simple test to estimate the permeability of the pore system for CO₂. For capillary suction, the weight was measured 0.2, 0.5, 1, 2, 4 and 24 h after placing the specimens in demineralized water at room temperature. Before weighting, the specimens were taken out of suction and placed for 2 s on a paper towel. After 30 s, the sample was returned to capillary suction. The water uptake was determined using the following equation:

$$\begin{aligned} \text{Water uptake} &= \Delta m / A \\ \Delta m: &\text{mass of sucked water in kg} \\ A: &\text{Exposed surface (40} \times \text{40 mm}^2\text{) in m}^2 \end{aligned} \quad (2)$$

The water uptake was then plotted against the square root of the immersion time. The slope of the straight line corresponds to the sorption coefficient *S*.

TGA is a reliable test method to determine the amount of CH and calcite within a sample quantitatively. The TGA measurements were carried out with STA 449 F3 Jupiter from Netzsch. With the heating rate 20 K/min, the samples were heated from 25 °C to 1050 °C. The evaluation was carried out with the program Netzsch Proteus. For evaluation, the mass loss between 400 and 500 °C was assigned to the dehydration of portlandite. Furthermore, the mass loss at a temperature ranging from 600 to 800 °C was assigned to the decomposition of calcite.

In order to compare the amount of portlandite (Ca(OH)₂) and calcite (CaCO₃) independent of the amount of free water, the percentage share of the two phases is related to the amount of hardened cement paste with the following equations.

$$\text{Ca(OH)}_2 = \frac{M(\text{Ca(OH)}_2)}{M(\text{H}_2\text{O})} \cdot \frac{\Delta w_{400-500^\circ\text{C}}}{100 - w_{110^\circ\text{C}}} \cdot 100 = \frac{74.0927}{18.01528} \cdot \frac{\Delta w_{400-500^\circ\text{C}}}{100 - w_{110^\circ\text{C}}} = 4.11 \cdot \frac{\Delta w_{400-500^\circ\text{C}}}{100 - w_{110^\circ\text{C}}} \quad (3)$$

$$\text{CaCO}_3 = \frac{M(\text{CaCO}_3)}{M(\text{H}_2\text{O})} \cdot \frac{\Delta w_{600-800^\circ\text{C}}}{100 - w_{110^\circ\text{C}}} \cdot 100 = \frac{100.0869}{1.01528} \cdot \frac{\Delta w_{600-800^\circ\text{C}}}{100 - w_{110^\circ\text{C}}} = 5.56 \cdot \frac{\Delta w_{600-800^\circ\text{C}}}{100 - w_{110^\circ\text{C}}} \quad (4)$$

3. Results and Discussion

3.1. Effect of Pre-Conditioning and RH during Accelerated Carbonation

Figure 5 shows the carbonation depth after 7 d. The label of the *x*-axis describes the binder type used (M1, M2 or M3), then the first number gives the RH percentage of pre-conditioning and the second number gives the RH percentage of accelerated carbonation. It can be stated that pre-conditioning at 50% RH led to higher carbonation rates compared to 65% RH (Figure 5 top). This is true for all test series, except M2 exposed to 57% RH during accelerated carbonation (Figure 5 top, middle green columns). However, the variation in the carbonation depth of M2 exposed to 57% RH during accelerated carbonation for pre-conditioning at either 50% and 65% RH is in the range of the scatter of individual measurements (see related error bars in Figure 5 top) and can thus be neglected. Furthermore, it can be stated that the effect of increased carbonation depths when pre-conditioning performed at 50% RH was more pronounced for specimens with OPC (M1) and slag (M3) than for binders with limestone fillers (M2), which is in line with the general conclusions of Leeman et al. [15]. The high scatter results from the well-known side-effect of mortar prisms: the side without formwork shows higher carbonation rates than the bottom side; see [32]. Eliminating the top and bottom sides would lead to less scatter and

to an even more pronounced distinction between different RH during pre-conditioning (Figure 5 bottom).

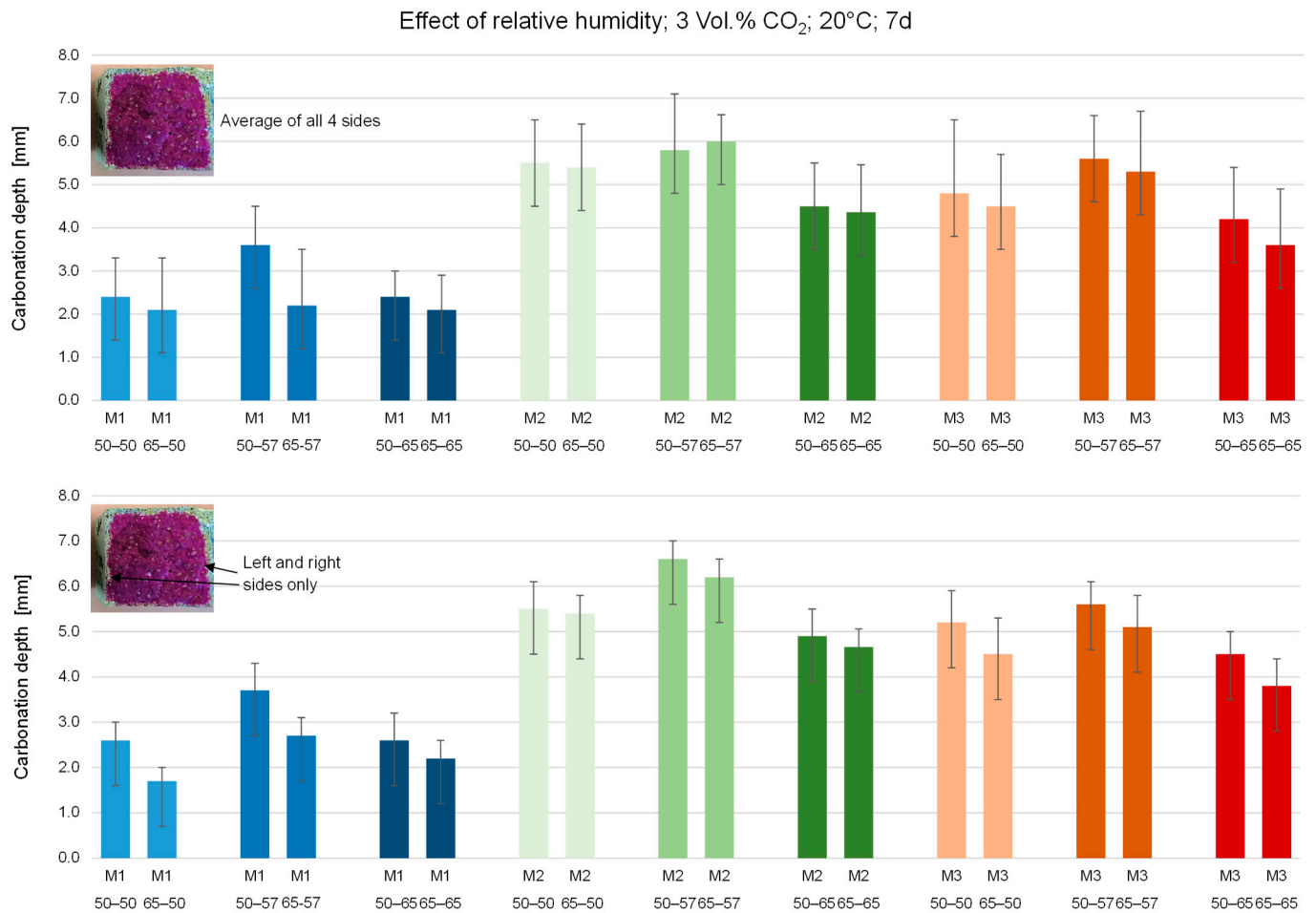


Figure 5. (Top): Carbonation depth determined at 7 d for accelerated conditions at 3% CO₂—readings on all four sides of the freshly broken specimen surface (see picture top left); (bottom): carbonation depth determined at 7 d for accelerated conditions at 3% CO₂—readings only on left and right sides of the specimen. Sample labelling: Mx-aa-bb: x = binder type, aa = Relative humidity during pre-conditioning, bb = Relative humidity during carbonation.

Figure 6 shows the carbonation depth up to 28 d under accelerated conditions for mortars with different binders (readings were taken on all four sides of the freshly broken specimen surface). The effect of pre-conditioning did not change over time. The mortar incorporating slag showed a slight deviation from the square-root time law. These results showed that pre-conditioning plays an important role in accelerated carbonation testing. Fourteen days, as suggested by [2], might be too short to reach equilibrium condition, especially for concrete and mortar specimens with low w/c ratio. Soja et al. [20,33] found that the pore structure is severely affected by storage conditions. This is indirectly confirmed by the sorption coefficients shown in Table 3. Pre-storage at 50% RH led to higher sorption coefficients, which further increased due to carbonation. Soja et al. [20], therefore, recommended to subtracting the effect of drying from the effect of carbonation.

Table 3. Sorption coefficients ($\text{kg}/(\text{m}^2 \cdot \text{h}^{0.5})$) before and after accelerated carbonation at 57% RH, 3 vol.% CO_2 , 20 °C and ambient, pressure, ACC = accelerated carbonation.

Exposure	M1 50–57	M1 65–57	M2 50–57	M2 65–57	M3 50–57	M3 65–57
Before carbonation	0.76	0.48	1.58	1.09	1.20	1.07
7 d ACC	0.85	0.63	2.43	2.21	1.46	1.49

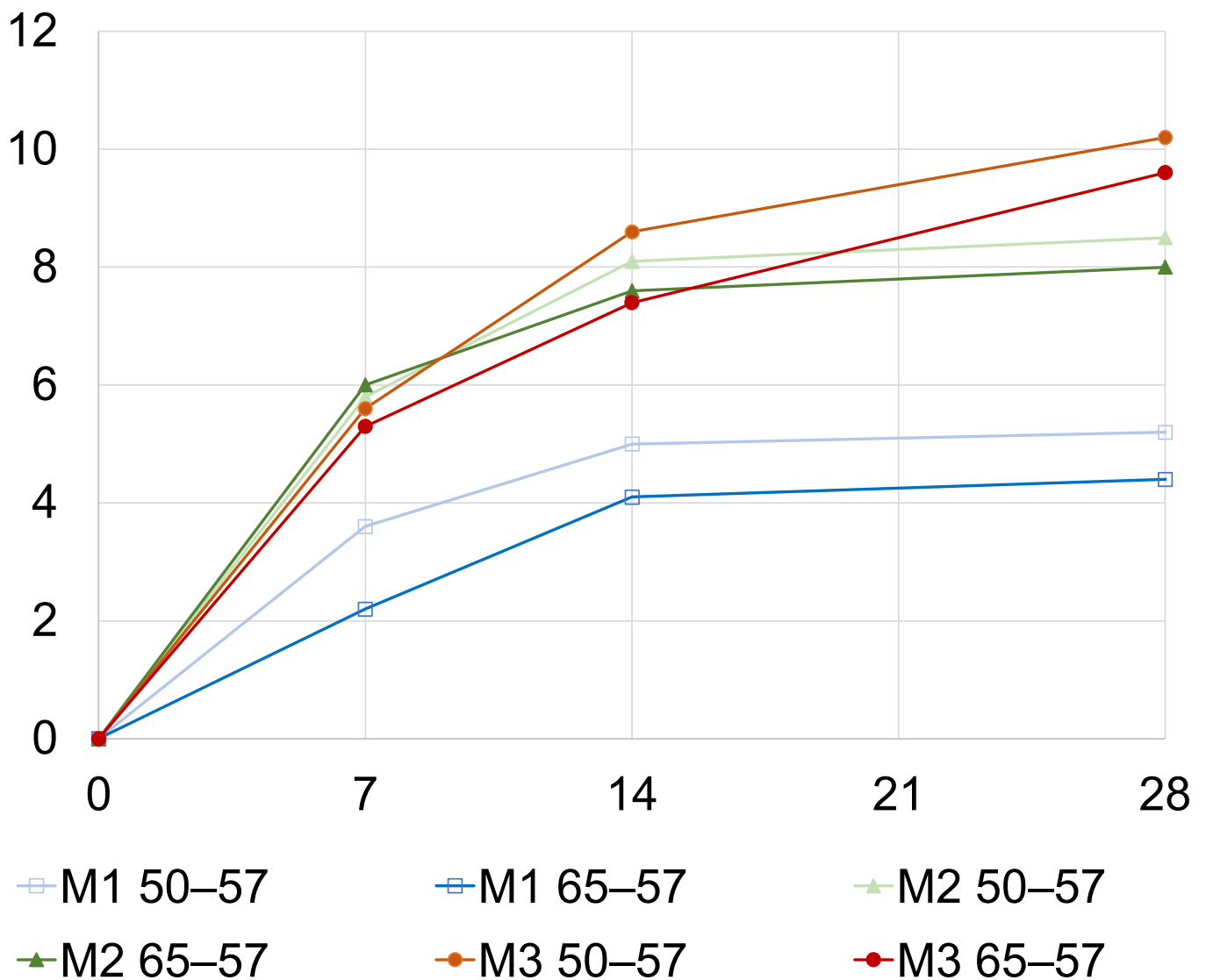


Figure 6. Carbonation depth of mortars with different binders pre-conditioned at either 50 or 65% RH and carbonated under accelerated conditions at 57% RH, 3 vol.% CO_2 , 20 °C and ambient pressure.

To discuss the effect of relative humidity during accelerated carbonation, the series pre-conditioned at 65% RH are further analyzed.

Figure 7 shows the changes in pore size distribution for all three mortars before and after 7 d of accelerated carbonation at 50% and 65% RH. For M1, the total porosity decreased from 12.9% to 10.3% and 10.5%, while, at the same time, a slight coarsening of the pore structure is observed as the peak of the pore size distribution clearly shifts to the right (see arrows in Figure 7a). For the mortar M2 with limestone filler, the same trend was observed. However, here, 65% RH led to increased coarsening while the effect of reduction in total porosity and the coarsening was more pronounced for the specimens stored at 50% RH during carbonation for the mixes with slag and OPC. As the mix with limestone

filler had the highest initial porosity, the findings of Leeman et al. [15] concerning capillary condensation as the reason for the different behavior can be confirmed. The impact of porosity also displays the carbonation depth. However, while the MIP measurements show a decrease in total porosity, the sorption coefficients increase for 50% RH and 65% RH (see Table 4). This could be due to near-surface micro-cracking due to carbonation shrinkage.

Table 4. Sorption coefficients ($\text{kg}/(\text{m}^2 \cdot \text{h}^{0.5})$) before and after accelerated carbonation at 50% and 65% RH, 3 vol.% CO_2 , 20 °C and ambient pressure, ACC = accelerated carbonation.

Exposure	M1	M2	M3
Before Carbonation	0.48	1.09	1.07
7d ACC 3% CO_2 and 50% RH	0.53	1.76	1.72
7d ACC 3% CO_2 and 65% RH	0.57	1.84	1.24

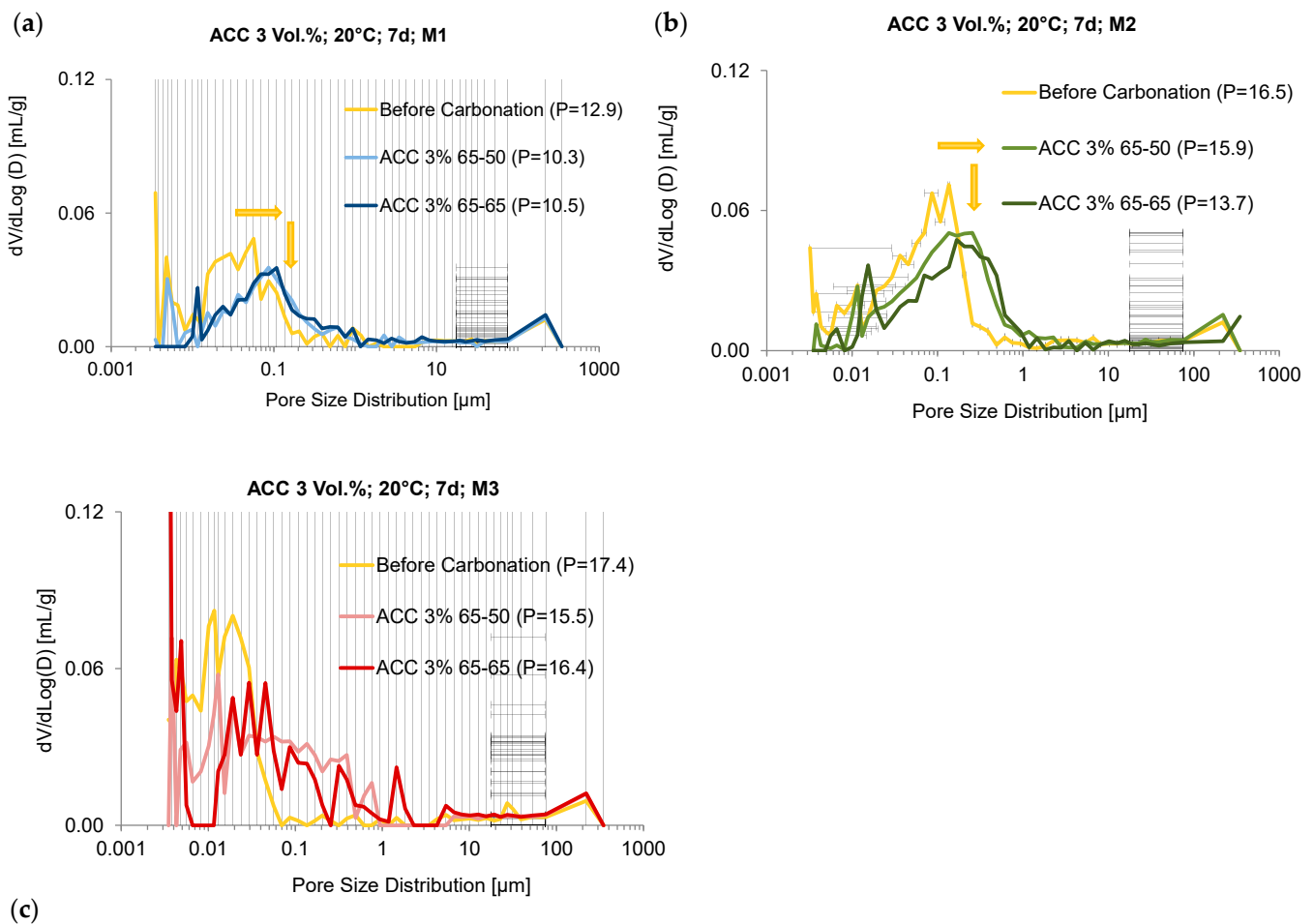


Figure 7. Pore Size Distribution before and after 7 d accelerated carbonation at atmospheric pressure and 3 vol.% CO_2 : (a) M1 (mortar with OPC); (b) M2 (mortar with limestone); (c) M3 (mortar with granulated blast furnace slag).

Table 5 shows the chemical changes observed with TGA. M1 incorporates 14% calcite before carbonation and almost 17% portlandite. Significant amounts of portlandite remain after a complete color change is observed with the spray test. Galan et al. [34] explain this phenomenon with the coating of portlandite crystals with a calcite film. Interestingly, within M3, portlandite is hardly consumed at all and the carbonation of C-S-H is pre-dominant.

Table 5. Comparison of mass loss and amount of portlandites and calcite at different ambient humidities for accelerated carbonation (3 vol.%) at pre-storage humidity 65%; 7d.

		Mass Loss (%)					% of Hardened Cement Paste	
		<110 °C	110–400 °C	400–500 °C	600–800 °C	20–1110 °C	CH	CaCO ₃
		Water	Ettringite, C-S-H	Portlandite	Calcite	Total Mass Loss		
M1	Before Carbonation	−2.7	−3.8	−1.7	−1.4	−10.2	7.2	8.2
	ACC 50% RH	−1.9	−2.8	−1.0	−5.6	−12.5	4.2	31.6
	ACC 65% RH	−0.4	−2.6	−0.9	−5.3	−9.9	3.5	29.4
M2	Before Carbonation	−1.2	−3.0	−1.4	−2.5	−9.2	5.8	13.9
	ACC 50% RH	−1.4	−2.7	−0.8	−7.3	−12.6	3.3	41.3
	ACC 65% RH	−1.4	−2.4	−0.7	−8.0	−13.0	3.0	45.2
M3	Before Carbonation	−2.0	−2.4	−0.6	−1.4	−6.5	2.6	8.0
	ACC 50% RH	−1.8	−2.5	−0.7	−3.1	−8.7	2.9	17.3
	ACC 65% RH	−1.4	−2.5	−0.8	−4.1	−9.6	3.4	23.2

As expected from the literature [12,35], high RH during carbonation promotes the formation of CaCO₃ from CH. The results are in line with the physical changes due to carbonation.

3.2. Effect of CO₂ Impact

The effect of different level of CO₂ exposure is investigated using natural carbonation after 84 d, 1 vol.% CO₂ after 7d, 3 vol.% CO₂ after 7 days and 3 vol.% CO₂ at 2 barg after 7 d, whereas all other exposure conditions are identical. The average values and the respective standard deviations of the carbonation depths of M2 read from the phenolphthalein indicator solution are shown in Table 6. The effect of additional gaseous pressure on mortar mixes 1 and 3 was not investigated.

Table 6. Carbonation depth of M1, M2 and M3 under different CO₂ exposures (RH during accelerated carbonation: 65%).

	Natural Carbonation 84 d		Accelerated Carbonation 7 d, 1 vol.% CO ₂		Accelerated Carbonation 7 d, 3 vol.% CO ₂		Accelerated Carbonation 7 d, 3 vol.% CO ₂ and 2 Barg	
	μ	σ	μ	σ	μ	Σ	M	σ
M1—50–65	0.8	0.5	1.0	0.7	2.4	0.6	-	-
M1—65–65	1.1	0.4	0.8	0.7	2.1	0.8	-	-
M2—50–65	1.4	0.4	2.3	0.9	4.5	1.0	6.8	1.2
M2—65–65	1.5	0.4	2.4	0.5	4.4	1.1	6.4	1.1
M3—50–65	1.9	0.7	2.1	0.6	4.2	1.2	-	-
M3—65–65	1.7	0.6	1.9	0.5	3.6	1.3	-	-

Pre-storage at 50% RH did not always lead to higher carbonation rates. However, the results are close together, indicating that interpretation is difficult here. With an increased CO₂ concentration and pressure, the relative humidity during pre-storage becomes more significant. Note that at the same time, the readings are also more accurate since the carbonation depth is deeper and, therefore, easier to measure. Consequently, pre-storage at 50% instead of 65% has the advantage that different carbonation resistances due to a mixed design can be more reliably distinguished.

The accelerated carbonation shows greater carbonation depths after 7 d than natural carbonation after 84 days. Thus, the increase in CO₂ concentration brings the desired effect, independent of the CO₂ content. Increasing the CO₂ concentration from 1 vol.% to

3 vol.% produces greater carbonation depths by a factor of 1.67 on average, which is close to the theoretical acceleration of 1.73. Additionally, adding 2 barg of pressurization to the same CO₂ concentration (3 vol.%) produces a further increase by a factor of 1.5. Increased carbonation impact led to higher carbonation of C-S-H and portlandite (Table 7). Here, portlandite also remained present in all samples.

Table 7. Comparison of mass loss for natural (“NAC”, 0.04 vol.% CO₂), and accelerated carbonation (“ACC”, 1 vol.% CO₂, 3 vol.% CO₂ and 3% plus 2 barg) at pre-storage at 65% RH; and 65% RH during carbonation.

	Mass Loss [%]					% of Hardened Cement Paste	
	<110 °C	110–400 °C	400–500 °C	600–800 °C	20–1110 °C	CH	CaCO ₃
	Water	Ettringite, C-S-H	Portlandite	Calcite	Total Mass Loss		
Before Carbonation	−1.2	−3.0	−1.4	−2.5	−9.2	5.8	13.8
NAC, 84 d	−1.6	−2.4	−0.8	−7.3	−12.6	3.2	41.0
ACC, 7d, 1%	−1.7	−2.6	−0.9	−6.4	−12.1	3.7	36.3
ACC, 7d, 3%	−1.4	−2.4	−0.7	−8.0	−13.0	3.0	45.2
P_ACC, 7d, 3%, 2 barg	−1.9	−2.4	−0.8	−8.4	−14.0	3.1	47.5

Based on the carbonation depths of the accelerated test series read by the color spray test after 7 days and the depth of the samples carbonated under natural conditions, the acceleration factors $D_{c, is}$ and correction factors in Table 8 were obtained.

Table 8. Carbonation coefficient k_{NAC} , theoretical and determined carbonation depth and correction factors for M1, M2 and M3 under different CO₂ exposure and varying pre-conditioning of either 50% or 65% RH.

	k_{NAC}	$D_{c, corr, 1\%} = k_{NAC} * \sqrt{\frac{7}{365}} * \sqrt{\frac{1}{0.04}} * 1.17$	$D_{c, is, 1\%}$	$D_{c, corr, 3\%} = k_{NAC} * \sqrt{\frac{7}{365}} * \sqrt{\frac{3}{0.04}}$	$D_{c, is, 3\%}$	Correction Factor 3% (NAC-ACC)
M1 50–65	1.67	1.3	1.3	1.97	2.4	1.22
M1 65–65	2.29	1.8	1.6	2.71	2.1	0.77
M2 50–65	2.92	2.3	2.3	3.45	4.5	1.30
M2 65–65	3.13	2.5	2.4	3.70	4.4	1.20
M3 50–65	2.92	2.3	2.6	3.45	4.2	1.22
M3 65–65	2.50	2.0	2.4	2.96	3.6	1.22

The theoretical acceleration factors according to Equation (1) for 1 vol.% and 3 vol.% CO₂ are 5.00 and 8.66, respectively. As can be seen in Table 8, using the correction factor of 1.17 proposed by [6] led to satisfying correlations for M1 and M2, while for M3, 1 vol.% CO₂ led to higher acceleration, and therefore, the correction factor might not be necessary. According to our results, a correction factor between 1.22 and 1.30 seems suitable for accelerated testing at 3 vol.% CO₂ and 65% RH. However, to determine and validate a correction factor suitable for concrete with SCMs, further studies should investigate a wide variety of concrete mixes at 3 vol.% CO₂ with the same boundary conditions as proposed in the standard. As the relative humidity affects the carbonation, the correction factor might increase.

4. Conclusions

For cementitious materials, carbonation usually leads to a reduction in total porosity and to an increase in strength. Carbonation depends on the amount of CO₂ partial and gaseous pressure and the relative humidity. The results on the ambient conditions during accelerated carbonation mainly confirm the results of earlier experiments and the resulting implementation in standards. The main objective of accelerated carbonation tests is to

receive reliable results in a short period of time and to overcome the long testing times required under natural conditions. New conclusions can be drawn based on this work regarding the pre-storage and the duration of the experiment.

Preconditioning for only the 14 d provided in DIN EN 12390-12:2020-04 was found to be too short of a time period to properly dry samples so that the effect of drying can be neglected. It is therefore recommended to increase this period and to shorten the curing time to receive reliable carbonation coefficients. During accelerated testing of the carbonation resistance, a relative ambient humidity of 57% is recommended since the highest carbonation rate is achieved here irrespective of the other conditions. The resulting higher carbonation depths are subjected to higher reading accuracy under otherwise identical measurement conditions. Regarding the duration of carbonation, the results of this work indicate that measurements after 7 d are always on the safe side and are therefore sufficient if the subsequent course is calculated according to the \sqrt{t} law. Thus, the duration of 70 d, as suggested by the current standard, can provide more precise information about the progress over time but is not necessary for a reliable classification of the carbonation resistance. Based on the results, a shortening of the test is an option. The comparison of the theoretical and the calculated acceleration factors shows the greatest correspondence at a CO₂ concentration of 1 vol.%. One advantage of higher acceleration, on the other hand, is the higher carbonation depths and thus easier readings. Changes in chemical composition and pore structure are comparable to the mere increase in CO₂ concentration. The results of the test specimens with pressurization also show reliable results, which encourages further research in this area. As minor deviations in temperature, RH and CO₂ concentration severely affect the results, data recording is recommended for fair interpretation of measurements.

Author Contributions: Conceptualization, C.T.; methodology, C.T.; validation, T.K.; formal analysis, T.K. and C.G.; investigation, J.K., B.G. and C.T.; resources, T.K. and C.G.; data curation, J.K., B.G. and C.T.; writing—original draft preparation, C.T.; writing—review and editing, C.T., T.K. and C.G.; visualization, J.K. and C.T.; supervision, T.K. and C.G.; project administration, C.T., B.G. and T.K.; funding acquisition, C.G. All authors have read and agreed to the published version of the manuscript.

Funding: This work has been supported by the German Research Foundation (DFG), project number 221646279. This support is gratefully acknowledged.

Institutional Review Board Statement: Not applicable.

Informed Consent Statement: Not applicable.

Data Availability Statement: Data are available from the authors on request.

Conflicts of Interest: The authors declare no conflict of interest.

References

1. Andersson, R.; Fridh, K.; Stripple, H.; Häglund, M. Calculating CO₂ uptake for existing concrete structures during and after service life. *Environ. Sci. Technol.* **2013**, *47*, 11625–11633. [[CrossRef](#)] [[PubMed](#)]
2. DIN EN 12390-12:2020-04; Testing Hardened Concrete—Part 12: Determination of the Carbonation Resistance of Concrete—Accelerated Carbonation Method. German Version EN 12390-12:2020. Deutsches Institut für Normung, Beuth Verlag: Berlin, Germany, 2020.
3. von Greve-Dierfeld, S.; Lothenbach, B.; Vollpracht, A.; Wu, B.; Huet, B.; Andrade, C.; Medina, C.; Thiel, C.; Gruyaert, E.; Vanoutrive, H.; et al. Understanding the carbonation of concrete with supplementary cementitious materials: A critical review by RILEM TC 281-CCC. *Mater. Struct.* **2020**, *53*, 136. [[CrossRef](#)]
4. Auroy, M.; Poyet, S.; le Bescop, P.; Torrenti, J.-M.; Charpentier, T.; Moskura, M.; Bourbon, X. Comparison between natural and accelerated carbonation (3% CO₂): Impact on mineralogy, microstructure, water retention and cracking. *Cem. Concr. Res.* **2018**, *109*, 64–80. [[CrossRef](#)]
5. Gehlen, C. Probabilistische Lebensdauerbemessung von Stahlbetonbauwerken-Zuverlässigkeitsbetrachtungen zur Wirksamen Vermeidung von Bewehrungskorrosion. Doctoral Thesis, RWTH Aachen, Aachen, Germany, 2000.
6. Hunkeler, F.; von Greve-Dierfeld, S. *Karbonatisierung von Beton und Korrosionsgeschwindigkeit der Bewehrung im Karbonatisierten Beton (Carbonation of Concrete and Reinforcement Corrosion Rate in Carbonated Concrete)*; Research Report Published by the Swiss Federal Roads Office VSS No. 696; Federal Roads Office: Bern Switzerland, 2019.

7. Galan, I.; Andrade, C.; Castellote, M. Natural and accelerated CO₂ binding kinetics in cement paste at different relative humidities. *Cem. Concr. Res.* **2013**, *49*, 21–28. [[CrossRef](#)]
8. Harrison, T.A.; Jones, M.R.; Newlands, M.D.; Kandasami, S.; Khanna, G. Experience of using the prTS 12390-12 accelerated carbonation test to assess the relative performance of concrete. *Mag. Concr. Res.* **2012**, *64*, 737–747. [[CrossRef](#)]
9. Phung, Q.T.; Maes, N.; Jacques, D.; Bruneel, E.; van Driessche, I.; Ye, G.; de Schutter, G. Effect of limestone fillers on micro-structure and permeability due to carbonation of cement pastes under controlled CO₂ pressure conditions. *Constr. Build. Mater.* **2015**, *82*, 376–390. [[CrossRef](#)]
10. Zou, D.; Liu, T.; Du, C.; Teng, J. Influence of Wind Pressure on the Carbonation of Concrete. *Materials* **2015**, *8*, 4652–4667. [[CrossRef](#)] [[PubMed](#)]
11. Steiner, S.; Lothenbach, B.; Borgschulte, A.; Winnefeld, T.P.F. Effect of relative humidity on the carbonation rate of portlandite, calcium silicate hydrates and ettringite. In Proceedings of the Internationale Baustofftagung (Ibausil), Weimar, Germany, 12–14 September 2018.
12. Steiner, S. Carbonation of Concrete Made from Limestone-Rich Cement: CO₂ Diffusivity and Alteration of Hydrate Phases. Ph.D. Thesis, Technische Universität Darmstadt, Darmstadt, Germany, 2020.
13. Elsalamawy, M.; Mohamed, A.R.; Kamal, E.M. The role of relative humidity and cement type on carbonation resistance of concrete. *Alex. Eng. J.* **2019**, *58*, 1257–1264. [[CrossRef](#)]
14. Papadakis, V.G. Fundamental modeling and experimental investigation of concrete carbonation. *ACI Mater. J.* **1991**, *88*, 363.
15. Leemann, A.; Moro, F. Carbonation of concrete: The role of CO₂ concentration, relative humidity and CO₂ buffer capacity. *Mat. Struct.* **2017**, *50*, 30. [[CrossRef](#)]
16. Russel, D.; Basheer, P.M.; Rankin, G.B.; Long, A.E. Effect of relative humidity and air permeability on prediction of the rate of carbonation of concrete. *Proc. Institut. Civil Eng.-Struct. Build.* **2001**, *146*, 319–326. [[CrossRef](#)]
17. de Ceukelaire, L.; van Nieuwenburg, D. Accelerated carbonation of a blast-furnace cement concrete. *Cem. Concr. Res.* **1993**, *23*, 442–452. [[CrossRef](#)]
18. Atiş, C.D. Accelerated carbonation and testing of concrete made with fly ash. *Constr. Build. Mater.* **2003**, *17*, 147–152. [[CrossRef](#)]
19. Rougeau, P. *Les re 'Sultats D'essais Croise 's AFREM «Essai de Carbonatation Accéléré», dans Compterendu des Journées Techniques, AFPC-AFREM Durabilité des Bétons, « Méthodes Recommandées pour la Mesure des Grandeurs Associées à la Durabilité»*; CERIB: Toulouse, France, 1997. (In French)
20. Soja, W.; Georget, F.; Maraghechi, H.; Scrivener, K. Evolution of microstructural changes in cement paste during environmental drying. *Cem. Concr. Res.* **2020**, *134*, 106093. [[CrossRef](#)]
21. *DIN EN 206:2017*; Beton Festlegung, Eigenschaften, Herstellung und Konformität. Beuth: Berlin, Germany, 2017.
22. Gehlen, C.; Thiel, C. Specification of building materials for in service durability. In Proceedings of the ICSBM 2019: 2nd International Conference of Sustainable Building Materials, Eindhoven, The Netherlands, 12–15 August 2019.
23. Thiel, C.; von Einfluss, C. CO₂-Druck und Feuchtegehalt auf das Porengefüge Zementgebundener Werkstoffe Während der Carbonatisierung. Ph.D. Thesis, Technische Universität München, Munich, Germany, 2023. (under review).
24. *DIN EN 480-5:2005-12*; Zusatzmittel für Beton, Mörtel und Einpressmörtel-Prüfverfahren-Teil_5: Bestimmung der kapillaren Wasseraufnahme. Deutsche Fassung EN_480-5:2005. Deutsches Institut für Normung, Beuth Verlag: Berlin, Germany, 2005.
25. Martys, N.S.; Ferraris, C.F. Capillary transport in mortars and concrete. *Cem. Concr. Res.* **1997**, *27*, 747–760. [[CrossRef](#)]
26. Panesar, D.K.; Francis, J. Influence of limestone and slag on the pore structure of cement paste based on mercury intrusion porosimetry and water vapour sorption measurements. *Constr. Build. Mater.* **2014**, *52*, 52–58. [[CrossRef](#)]
27. Thienel, K.C.; Schmidt-Döhl, F.; Feldrappe, V. In-Situ Tests on Existing LWAC Structures. In Proceedings of the Second International Conference on Structural Lightweight Aggregate Concrete, Kristiansand, Norway, 18–22 June 2000.
28. Villain, G.; Thiery, M. Gammadensimetry: A method to determine drying and carbonation profiles in concrete. *NDT E Int.* **2006**, *39*, 328–337. [[CrossRef](#)]
29. Castellote, M.; Andrade, C.; Turrillas, X.; Campo, J.; Cuello, G.J. Accelerated carbonation of cement pastes in situ monitored by neutron diffraction. *Cem. Concr. Res.* **2008**, *38*, 1365–1373. [[CrossRef](#)]
30. Thiel, C.; Gehlen, C. On the determination of carbonation in cementitious materials. In Proceedings of the International Conference on Sustainable Materials Systems and Structures (SMSS2019) Durability, Monitoring and Repair of Structures, Rovinj, Croatia, 20–22 March 2019; Baričević, A., Rukavina, M.J., Damjanović, D., Guadagnini, M., Eds.; ISBN 978-2-35158-217-6.
31. Martens-Menzel, R.; Harwardt, L.; Krauss, J. *Maßanalyse: Titrationen mit Chemischen und Physikalischen Indikationen*; De Gruyter: Berlin, Germany; Boston, MA, USA, 2022.
32. Vanoutrive, H.; van den Heede, P.; Alderete, N.; Andrade, C.; Bansal, T.; Camões, A.; Cizer, Ö.; de Belie, N.; Ducman, V.; Etxeberria, M.; et al. Report of RILEM TC 281-CCC: Outcomes of a round robin on the resistance to accelerated carbonation of Portland, Portland-fly ash and blast-furnace blended cements. *Mater. Struct.* **2022**, *55*, 99. [[CrossRef](#)]
33. Soja, W. Carbonation of Low Carbon Binders. Ph.D. Thesis, EPFL, Lausanne, Switzerland, 2019. [[CrossRef](#)]

-
34. Galan, I.; Glasser, F.P.; Baza, D.; Andrade, C. Assessment of the protective effect of carbonation on portlandite crystals. *Cem. Concr. Res.* **2015**, *74*, 68–77. [[CrossRef](#)]
 35. Steiner, S.; Lothenbach, B.; Proske, T.; Borgschulte, A.; Winnefeld, F. Effect of relative humidity on the carbonation rate of portlandite, calcium silicate hydrates and ettringite. *Cem. Concr. Res.* **2020**, *135*, 106116. [[CrossRef](#)]